

# Aluminum Impregnation into Mesoporous Silica Molecular Sieves for Catalytic Application to Friedel–Crafts Alkylation

Shinae Jun and Ryong Ryoo<sup>1</sup>

*Materials Chemistry Laboratory, School of Molecular Science-BK21, Korea Advanced Institute of Science and Technology, Taejeon, 305-701, Korea*

Received January 12, 2000; revised July 7, 2000; accepted July 19, 2000

The catalytic activity of mesoporous molecular sieves for Friedel–Crafts alkylation of benzene, toluene, and *m*-xylene with benzyl alcohol was measured with three different types of materials, KIT-1 (disordered three-dimensional channel network), MCM-41 (hexagonal packing of one-dimensional channels), and MCM-48 (cubic *Ia3d* structure composed of two independent three-dimensional channel systems). Aluminum was incorporated into the mesoporous materials by various routes such as direct syntheses, grafting of the Al species with anhydrous AlCl<sub>3</sub>, and impregnation with an aqueous solution of AlCl<sub>3</sub>. The catalytic activity was analyzed with respect to the effects of the preparation methods, channel structures, and Al content. It turned out that postsynthesis impregnation was the most effective means for increasing the catalytic activity. The three types of mesoporous materials exhibited approximately the same surface character with regard to the catalytic reaction, independent of the different structures and synthesis conditions. Magic angle spinning <sup>27</sup>Al NMR spectroscopy of the impregnated samples indicated that the coordination of the Al sites thus generated lost the tetrahedral symmetry upon complete dehydration, supporting the possibility of three-coordinated catalytic sites. © 2000 Academic Press

**Key Words:** mesoporous materials; silica; Al incorporation; alkylation activity; acid catalysis.

## INTRODUCTION

Friedel–Crafts alkylation is an important means for attaching alkyl chains to aromatic rings. The alkylation is traditionally performed with alkyl halides using Lewis acid catalysts such as HF and AlCl<sub>3</sub> or with alcohols using Brønsted acids, typically H<sub>2</sub>SO<sub>4</sub>. However, the homogeneous catalysts are not easily separable after the reaction or cause large amounts of acid waste generation. Active research has been directed at substituting the traditional homogeneous catalysts with heterogeneous acid catalysts such as clay minerals and zeolites (1). For example, montmorillonite supporting zinc and nickel chloride was reported to show high catalytic activity in Friedel–Crafts alkylation re-

actions (2–4). The H<sup>+</sup> ion type of zeolite β was also reported to be a good catalyst for the alkylation (5).

The preparation of solid acid catalysts was extended to mesoporous molecular sieves in an attempt to remove the diffusion limitation with small zeolite pores. For example, the aluminosilicate form of MCM-41 (6, 7) was found to show a good catalytic activity for Friedel–Crafts alkylation of 2,4-di-*tert*-butylphenol (8). The catalytic activity of the mesoporous aluminosilicate increased after the ion exchange of Fe<sup>3+</sup>, due to the generation of Lewis acid sites (9). Aluminum-containing SBA-15 exhibited ion-exchange capacity and catalytic activity for cumene cracking, which was a reverse alkylation process (10, 11). Other studies have led to the conclusion that Al incorporation into the mesoporous silica materials can generate weak Brønsted acid sites that are suitable for reactions requiring mild acidity (12) such as acetalization (13), Beckmann rearrangement (14), and aldol condensations (15).

Recently, various routes have been developed for Al incorporation to MCM-41 (16–19). The mesoporous aluminosilicate molecular sieves thus obtained are constructed with pore walls formed by the disordered atomic arrangement. Consequently, the mesoporous walls have more or less different degrees of silicate cross-linking, locations of Al sites, and bond angles at the Al sites, depending on synthesis conditions. The noncrystalline nature of the mesopore walls gives the mesoporous materials various catalytic activities. It is therefore important to correctly assess the catalytic activity depending on not only the Al content but also the synthesis conditions.

The present study was undertaken in order to optimize synthesis conditions for the mesoporous aluminosilicate molecular sieves, so that we can obtain the highest possible catalytic activities for Friedel–Crafts alkylation reactions. Mesoporous molecular sieves with three different channel structures, MCM-41 (hexagonal packing of one-dimensional channels), MCM-48 (cubic *Ia3d* composed of two independent three-dimensional channel systems), and KIT-1 (disordered three-dimensional channel network), were obtained by following synthesis procedures reported

<sup>1</sup> To whom correspondence should be addressed. E-mail: rryoo@sorak.kaist.ac.kr.

in the literature (20–23). The Al content in the mesoporous materials was changed by the addition of sodium aluminate into the synthesis reaction mixture. This synthesis procedure is designated as “direct synthesis.” The Al incorporation was also performed by two postsynthesis routes designated as “grafting” and “impregnation” methods. The grafting method involved binding Al species irreversibly onto the surface of pore walls through reaction with  $\text{AlCl}_3$  in anhydrous ethanol solution (24). The impregnation method involved evaporating water after slurrying mesoporous silica in an aqueous solution of  $\text{AlCl}_3$ , which was developed during the course of the present work (25). The catalytic activity of these mesoporous materials after calcination was investigated for Friedel–Crafts alkylation of benzene, toluene, and *m*-xylene, using benzyl alcohol as the alkylation agent.

## EXPERIMENTAL

### 1. Synthesis of Pure Silica Mesoporous Molecular Sieves

**1.1. KIT-1.** KIT-1 silica was obtained by following the synthesis procedure reported in Refs. 20 and 21 using cetyltrimethylammonium chloride (CTMACl) as the surfactant, an aqueous solution of sodium silicate with  $\text{Na}/\text{Si} = 0.5$  as a silica source, and ethylenediaminetetraacetic acid tetrasodium salt ( $\text{EDTANa}_4$ ) as a salt except for the modification of mixing modes. Distilled water and  $\text{EDTANa}_4$  (Acros, 99%) were added to the surfactant solution (Aldrich, 25 wt% CTMACl in  $\text{H}_2\text{O}$ ) in a polypropylene (PP) bottle. This mixture, possessing the molar composition of 1 CTMACl:5  $\text{EDTANa}_4$ :240  $\text{H}_2\text{O}$ , was stirred with a magnetic stirrer until the solution became homogeneous. To this solution was rapidly added the silica source (2.4 mass%  $\text{Na}_2\text{O}$ , 9.2 mass%  $\text{SiO}_2$ , 88.4 mass%  $\text{H}_2\text{O}$ ). Immediately, the mixture was vigorously shaken for about 2 min at room temperature. Stirring was continued for 1 h with a magnetic stirrer. The resultant mixture had a molar composition of 5  $\text{SiO}_2$ :1.25  $\text{Na}_2\text{O}$ :1 CTMACl:5  $\text{EDTANa}_4$ :400  $\text{H}_2\text{O}$ . The mixture was heated in an oven at 373 K for 1 d. The pH of the mixture in the PP bottle was adjusted to 10 with acetic acid after the mixture was cooled to room temperature. The mixture was heated again at 373 K for 5 d. After the 5-d heating period, the pH of the reaction mixture was adjusted again to 10 with acetic acid at room temperature. Product was filtered after the reaction mixture was heated for 1 d at 373 K. The product was washed with doubly distilled water, dried at 393 K, and stored until further use.

**1.2. MCM-41.** Highly ordered MCM-41 silica sample was obtained by following a synthesis method using CTMABr–cetyltriethylammonium bromide (CTEABr) mixtures (22). The same silica source used for KIT-1 was combined with an aqueous solution of CTEABr–CTMABr

at room temperature, and the resultant mixture was shaken vigorously, in the same way as for KIT-1. The molar composition of the starting mixture was 0.8 CTEABr:0.2 CTMABr:4  $\text{SiO}_2$ :1  $\text{Na}_2\text{O}$ :400  $\text{H}_2\text{O}$ . The synthesis of MCM-41 was carried out by repeating the reactant heating at 373 K and the pH adjustment, in the same way as for KIT-1, except that the second heating period was changed to 2 d instead of 5 d.

**1.3. MCM-48.** High-quality MCM-48 sample was prepared with CTMABr and  $\text{C}_{12}\text{H}_{25}\text{O}(\text{C}_2\text{H}_4\text{O})_4\text{H}$  (Brij 30, Aldrich), following a synthesis method using cationic–nonionic surfactant mixtures (23). Briefly, an aqueous solution containing the two surfactants was mixed with the same silica source and in the same way as for MCM-41 and KIT-1 syntheses. The molar composition of the starting mixture was 5.0  $\text{SiO}_2$ :1.25  $\text{Na}_2\text{O}$ :0.85 CTMABr:0.15 Brij 30:400  $\text{H}_2\text{O}$ . This mixture was heated for 60 h at 373 K. After cooling to room temperature, the reaction mixture was neutralized with acetic acid that was equivalent to 60% of the Na content in the reaction mixture. The addition of the acetic acid was carried out drop by drop with magnetic stirring. The reaction mixture after the neutralization was heated again for 2 d at 373 K.

### 2. Aluminum Incorporation

**2.1. Direct synthesis.** The direct synthesis of KIT-1 in the aluminosilicate form was performed in the same way as for the pure silica form, except for the addition of an aqueous solution containing sodium aluminate. The addition of the alumina source was carried out drop by drop with vigorous stirring, after the reaction mixture with the molar composition of 5  $\text{SiO}_2$ :1.25  $\text{Na}_2\text{O}$ :1 CTMACl:5  $\text{EDTANa}_4$ :400  $\text{H}_2\text{O}$  was stirred for 1 h at room temperature. After further mixing for 1 h, the resulting gel mixture was heated at 373 K. The mixture had the molar composition of 5  $\text{SiO}_2$ :2.5/ $x$   $\text{Al}_2\text{O}_3$ :(1.25 + 5/ $x$ )  $\text{Na}_2\text{O}$ :1 CTMACl:5  $\text{EDTANa}_4$ :400  $\text{H}_2\text{O}$ , where  $x$  was the Si/Al ratio. The remainder of the synthesis procedure is the same as that described for the synthesis of pure silica material (20, 21).

**2.2. Grafting method.** This method is a postsynthesis route to Al incorporation developed in our earlier work (24). Briefly, as-synthesized silica forms of MCM-41 (22), MCM-48 (23), and KIT-1 (20, 21) samples were washed with an ethanol–hydrochloric acid mixture (24) to remove the surfactant. The samples after washing were immediately dried in an oven at 413 K. Dried samples were then grafted with Al species while being slurried in an absolute ethanol solution of the anhydrous  $\text{AlCl}_3$  (Junsei, 98%). Because the Si/Al ratio of products is lower than those for reactants,  $\text{AlCl}_3$  was used in excess (24). The samples after the treatment with  $\text{AlCl}_3$  were washed with absolute ethanol, dried, and calcined in air.

**2.3. Impregnation method.** The surfactant was removed from the as-synthesized silica samples using ethanol-HCl in the same way as in Section 2.2. Samples were slurried in an aqueous solution of AlCl<sub>3</sub> for about 30 min at room temperature. The solution was then completely evaporated in a drying oven at 353 K. Dried samples were then calcined in air.

### 3. Characterization

Elemental analysis for Si/Al ratios was performed with inductively coupled plasma (ICP) emission spectroscopy (Shimadzu, ICPS-1000III). The X-ray powder diffraction (XRD) pattern was measured for calcined samples at room temperature using a Rigaku Miniflex instrument (Cu K $\alpha$  source, 450 W). The N<sub>2</sub> adsorption isotherm was measured at liquid N<sub>2</sub> temperature with a Micromeritics instrument (ASAP 2010). The specific surface area was calculated using the standard BET method. The pore size distribution was calculated using the BJH algorithm (26) after calibration as proposed by Kruk, Jaroniec, and Sayari (27). The magic angle spinning (MAS) <sup>27</sup>Al NMR spectrum was obtained at 296 K with a Bruker AM 300 instrument operating at 78.2 MHz. Typically, the NMR spectrum was obtained with radio frequency pulses for 1.8  $\mu$ s with 3.0-s recycle delays. The sample was spun at 3.5 kHz.

### 4. Catalytic Reaction

Calcined mesoporous samples were converted to the H<sup>+</sup> form through NH<sub>4</sub><sup>+</sup> ion exchange and subsequent calcination. Approximately 0.2 g of sample was placed in 100 ml of aqueous 5  $\times$  10<sup>-4</sup> M NH<sub>4</sub>NO<sub>3</sub> solution. After being stirred for 15 min at room temperature with a magnetic stirrer, the solution was filtered. The slurry-filtration treatment was repeated three times in all, in order to maximize the NH<sub>4</sub><sup>+</sup> ion exchange. The ion-exchanged sample was calcined in air at 823 K.

Catalytic activity was measured in the liquid phase with vigorous magnetic stirring under refluxing conditions: 353 K for benzylation of benzene, 383 K for toluene, and 411 K for *m*-xylene. Typical mole ratios between reactants in solution and Al in catalyst were 1 benzene : 0.025 benzyl alcohol : 0.65  $\times$  10<sup>-3</sup> Al, 1 toluene : 0.05 benzyl alcohol : 1.3  $\times$  10<sup>-3</sup> Al, and 1 *m*-xylene : 0.05 benzyl alcohol : 0.26  $\times$  10<sup>-3</sup> Al, respectively. The mole ratio for benzene corresponded to the addition of 0.17 g of catalyst with Si/Al = 19 into a mixture of 34.4 mL of benzene and 0.5 mL of benzyl alcohol. The benzene and catalyst mixture was stirred and preheated to the reaction temperature, prior to the addition of benzyl alcohol. The conversion of benzyl alcohol was analyzed by gas chromatography (HP 5980, equipped with a Carbowax 20M column at 443 K).

## RESULTS AND DISCUSSION

The XRD patterns for MCM-41, MCM-48, and KIT-1 samples obtained in the present work are shown in Fig. 1. The XRD patterns for pure silica forms of MCM-41 and MCM-48 show more than five resolved diffraction lines, indicating highly ordered structures. The XRD patterns for aluminosilicate MCM-41 and MCM-48 prepared by the direct synthesis procedures show poorly resolved lines, indicating loss of structural order compared with silica materials (28). The loss of structural order is a consequence of branching the MCM-41 channels at random. Unlike the case with direct synthesis, aluminosilicate samples obtained by postsynthesis routes exhibited highly ordered structures similar to those for the pure silica forms. The postsynthesis samples exhibited a narrow pore size distribution as represented by the MCM-48 data in Fig. 2. The pore size at the maximum of the distribution peak corresponded to approximately 3.8 nm in pore diameter, independent of structures of the three kinds of materials as given in Table 1. The BET surface areas were approximately 1000 m<sup>2</sup> g<sup>-1</sup>, similar to those of the high-quality mesoporous materials reported in our previous studies.

The structural difference for MCM-41 between direct synthesis and postsynthesis Al incorporation makes it difficult to investigate the intrinsic effects for the surface catalytic activity coming from the different Al incorporation

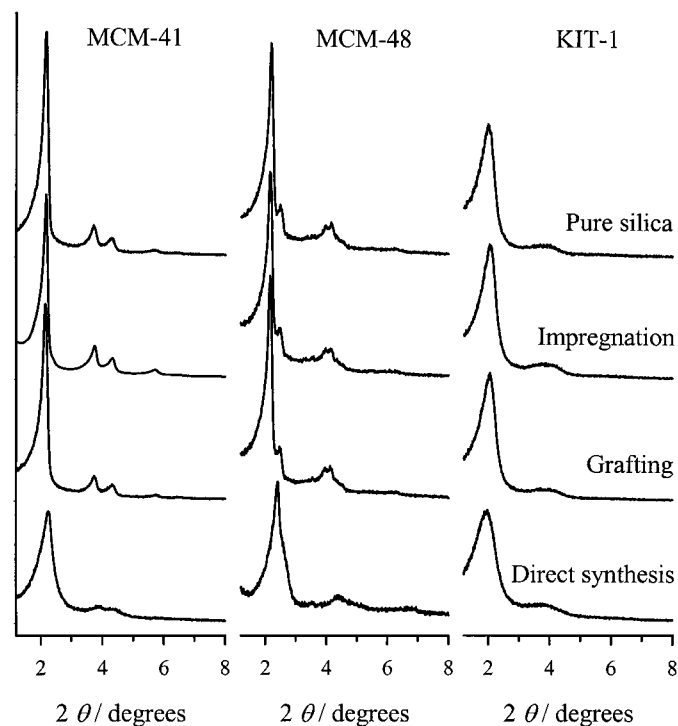


FIG. 1. XRD patterns for mesoporous molecular sieves after calcination. Except for the pure silica samples, all samples have the same Si/Al ratio of 19.

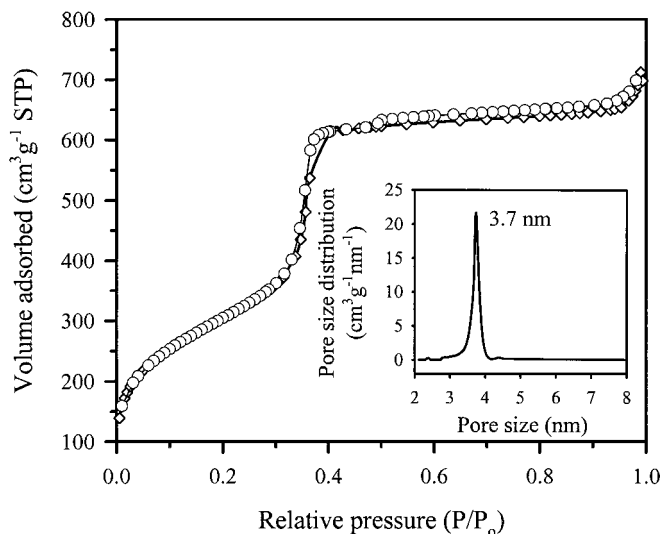


FIG. 2.  $N_2$  adsorption-desorption isotherms at 77 K for MCM-48 (Si/Al = 19) obtained by  $AlCl_3$  impregnation. Inset: the pore size distribution corresponding to the adsorption branch (calculated as described in Ref. 22).

procedures. The disordered MCM-41 material can exhibit significantly higher catalytic activity due to the facile diffusion through the branched channels wherever the catalytic activity is affected by channel blockage. In order to prevent this complication, we chose KIT-1 samples instead of MCM-41 for the investigation of the effects of various Al incorporation routes on the catalytic activity. All KIT-1 samples prepared in the present work had fully disordered and branched channel structures regardless of whether they were prepared in the aluminosilicate forms by direct synthesis or by postsynthesis routes after synthesis in the pure silica form, as shown in Fig. 1.

Figure 3 shows the catalytic activity of KIT-1 for the Friedel-Crafts alkylation of benzene. The catalytic reaction gave the monoalkylated product, dibenzylmethane, as a major product under the present reaction conditions us-

TABLE 1

Primary Mesopore Size and BET Surface Area for Mesoporous Molecular Sieves Prepared by  $AlCl_3$  Impregnation

	Si/Al ratio	$d$ spacing <sup>a</sup> (nm)	Pore diameter (nm)	BET area ( $m^2 g^{-1}$ )
MCM-41	19	4.0	3.7	1004
	38	4.0	3.8	1050
KIT-1	9	3.8	3.6	967
	19	3.7	3.6	956
	38	3.9	3.8	1021
	60	3.8	3.7	996
MCM-48	19	3.8	3.7	957
	38	4.0	3.9	1116

<sup>a</sup>  $d_{100}$  spacing for MCM-41;  $d$  spacing corresponding to the main XRD peak for KIT-1; and  $d_{210}$  spacing for MCM-48.

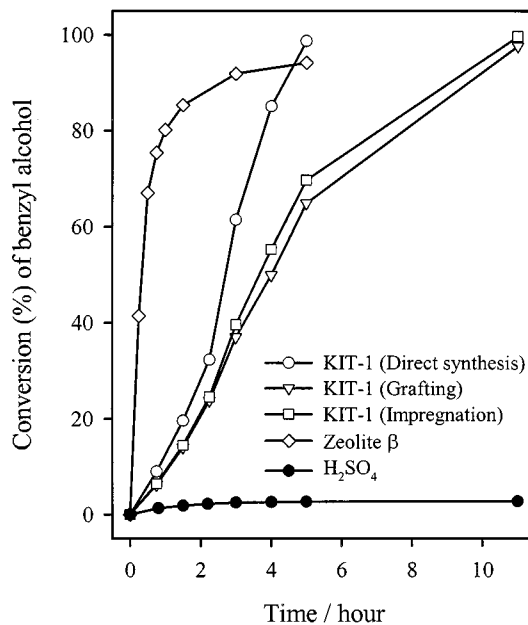
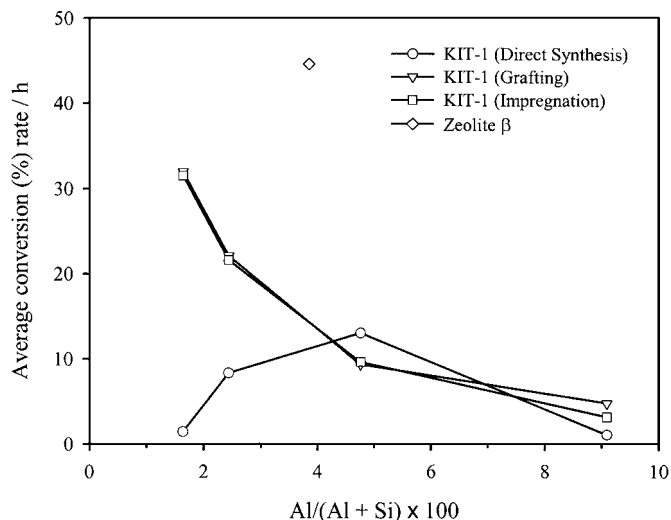


FIG. 3. Conversion (%) of benzyl alcohol for Friedel-Crafts alkylation of benzene plotted against reaction time: (○) KIT-1 (Si/Al = 19) by direct synthesis, (▽) KIT-1 (Si/Al = 19) by grafting method, (□) KIT-1 (Si/Al = 19) by impregnation, (◇) zeolite  $\beta$  (Si/Al = 25), and (●)  $H_2SO_4$ . The reaction mixture consisted of 34.4 ml of benzene and 0.50 ml of benzyl alcohol under reflux conditions at 353 K. The amount of catalyst was 0.17 g of KIT-1, 0.21 g of zeolite  $\beta$ , and 0.014 g of  $H_2SO_4$ .

ing benzene in excess. The concentration of the dialkylated product, dibenzylbenzene, corresponded to less than 20% of the total conversion of the benzyl alcohol until the conversion reached 90%. In Fig. 3, the total conversion of benzyl alcohol over three KIT-1 (Si/Al = 19) samples is plotted as a function of reaction time. As shown in Fig. 3, the two postsynthesis samples gave more or less slow conversion than the direct synthesis sample. Directly synthesized KIT-1 gave a 90% conversion to products within 6 h. The catalytic activity for KIT-1 was much higher than that of sulfuric acid catalyst, based on the comparison between the same number of  $H_2SO_4$  molecules and the same total number of Al sites. However, the catalytic activity was still much lower than that of zeolite  $\beta$  (VALFOR, Si/Al = 25).

In Fig. 4, various catalyst samples are compared with each other in terms of the average rate obtained during the initial 60% conversion of benzyl alcohol. As Fig. 4 shows, the catalytic activity depended very much on not only the preparation methods but also the Al content. The result shows that the catalytic activities of the postsynthesis samples were very similar to each other. The catalytic activities increased monotonously with the decrease in the Al content throughout the entire range of investigation:  $Al/(Al + Si) = 1.6-9.1$ . On the other hand, the direct synthesis samples exhibited a very different trend of activity against the Al content. Catalytic activities of the direct synthesis samples increased first and then decreased with the decrease in the Al



**FIG. 4.** Average conversion rate ( $\% \text{ h}^{-1}$ ) of benzyl alcohol during the initial 60% conversion. Reaction conditions are the same as in Fig. 3. The number  $100\% \text{ h}^{-1}$  in the ordinate corresponds to the conversion of 38 benzyl alcohol molecules per total Al site per hour.

content. At low Al content, the catalytic activities of post-synthesis samples were several times higher than those of directly synthesized samples. The high catalytic activity was not due to the effect of remaining chlorine, as the ICP analysis detected no significant chlorine content. Moreover, we confirmed that only about 20% of the catalytic activity was lost when  $\text{Al}(\text{NO}_3)_3$  was used instead of  $\text{AlCl}_3$  for catalyst preparation.

The various catalytic activities of the mesoporous materials reflect changes in the location of the Al sites and acidic strength depending on the Al content and the Al incorporation methods. Low catalytic activities at the high Al content are reasonable from the progressively increasing possibilities for the agglomeration into oxide domains as the Al content increases. The agglomeration is expected to occur particularly when a large amount of Al is deposited onto the silica pore walls during the impregnation treatments. Therefore, it is reasonable that the catalytic activity per Al site would increase with the decrease in the Al content. The results in Fig. 4 for postsynthesis samples show good agreement with this reasoning. However, as described above, the catalytic activity of directly synthesized samples shows a large decrease as the Al content decreased. This result suggests that many of the Al sites, in the case of the direct synthesis, became located inside the pore walls with the decrease in the Al content. These active sites would be difficult for reactants to access.

Figures 5 and 6 show the results for Friedel-Crafts benzoylation of toluene and *m*-xylene, respectively. The catalyst was the same impregnation KIT-1 ( $\text{Si}/\text{Al} = 19$ ) sample used to give the result shown in Fig. 3. The results in Figs. 5 and 6 indicate that the alkylation reaction can take place easily

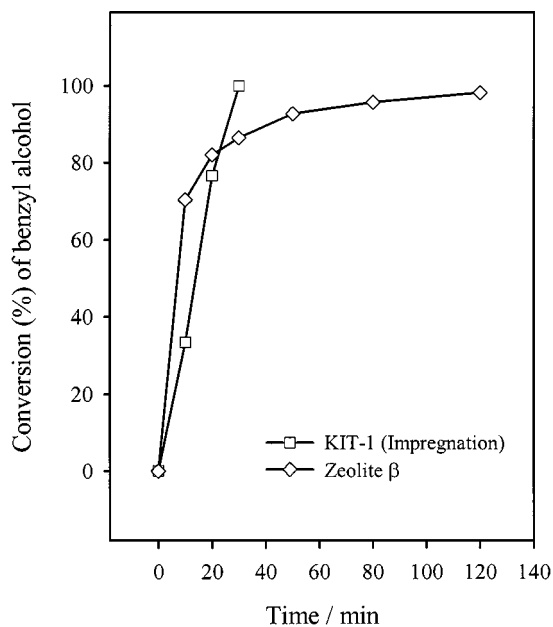


**FIG. 5.** Conversion (%) of benzyl alcohol for Friedel-Crafts alkylation of toluene plotted against reaction time: ( $\square$ ) KIT-1 ( $\text{Si}/\text{Al} = 20$ ) by  $\text{AlCl}_3$  impregnation, and ( $\diamond$ ) zeolite  $\beta$  ( $\text{Si}/\text{Al} = 25$ ). The reaction mixture consisted of 10.07 ml of toluene and 0.50 ml of benzyl alcohol under reflux conditions at 383 K. The amount of catalyst was 0.17 g of KIT-1 and 0.21 g of zeolite  $\beta$ .

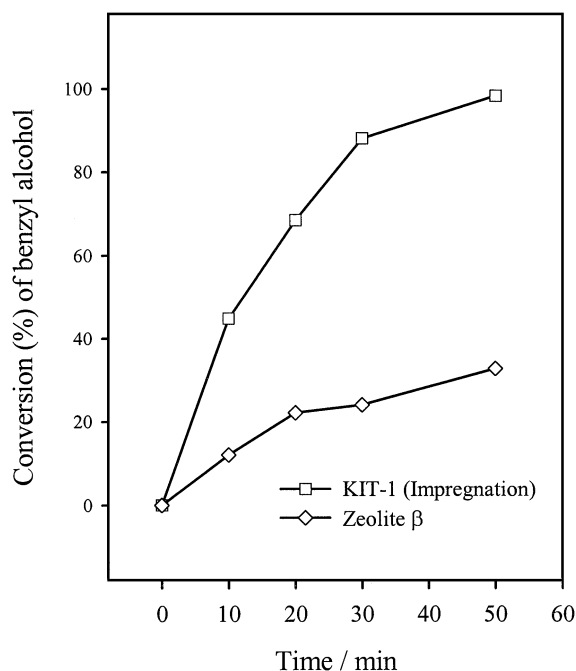


**FIG. 6.** Conversion of benzyl alcohol for Friedel-Crafts alkylation of *m*-xylene plotted against reaction time: ( $\square$ ) KIT-1 ( $\text{Si}/\text{Al} = 20$ ) by  $\text{AlCl}_3$  impregnation, and ( $\diamond$ ) zeolite  $\beta$  ( $\text{Si}/\text{Al} = 25$ ). The reaction mixture consisted of 14.0 ml of *m*-xylene and 0.59 ml of benzyl alcohol under reflux conditions at 411 K. The amount of catalyst was 0.17 g of KIT-1 and 0.21 g of zeolite  $\beta$ .

with toluene and *m*-xylene, which have electron-donating methyl groups on the benzene ring. The mesoporous catalyst gave even better results than zeolite  $\beta$  for the Friedel-Crafts reaction of the methyl-substituted aromatic compounds.

In order to investigate if there are any effects that may be attributed to differences in channel structures or the nature of frameworks, we have measured the catalytic activities of MCM-41 and MCM-48 after the incorporation of the same amount of Al (Si/Al = 19 or 38) following the same impregnation method as that used for KIT-1. The results are compared with those for KIT-1 in Table 2. As Table 2 shows, no systematic difference has been found between the samples. That is, the MCM-41 structure, which was composed of a one-dimensional channel system, showed no significant decrease in the catalytic activity compared with the three-dimensionally interconnected channel structures of KIT-1 and MCM-48. In fact, the catalytic activity depended more significantly on the details of synthesis conditions used to obtain silica forms rather than their structural differences. For example, the result for MCM-48 given in Table 2 was obtained from a sample that was synthesized using the surfactant mixture of CTMABr and Brij 30 (22). Other MCM-48 samples synthesized using only the cationic surfactant exhibited a much lower catalytic activity than that shown in Table 2. The low activity may be attributed to the deposition of amorphous silica layers (29) at the external surface of the MCM-48 particles.

Figure 7 shows MAS  $^{27}\text{Al}$  NMR spectra for KIT-1 samples, into which the Al was incorporated by postsynthesis impregnation. The MAS  $^{27}\text{Al}$  NMR spectra for the fully hydrated samples in Fig. 7 show two broad peaks, which can be assigned to the Al sites with tetrahedral and octahedral symmetries, respectively. The octahedral peak increased in intensity as the Al content increased, consistent with the decrease in the catalytic activity per Al in the postsynthesis samples. It is noteworthy that the NMR peaks almost disappeared after the samples were completely dehydrated. This

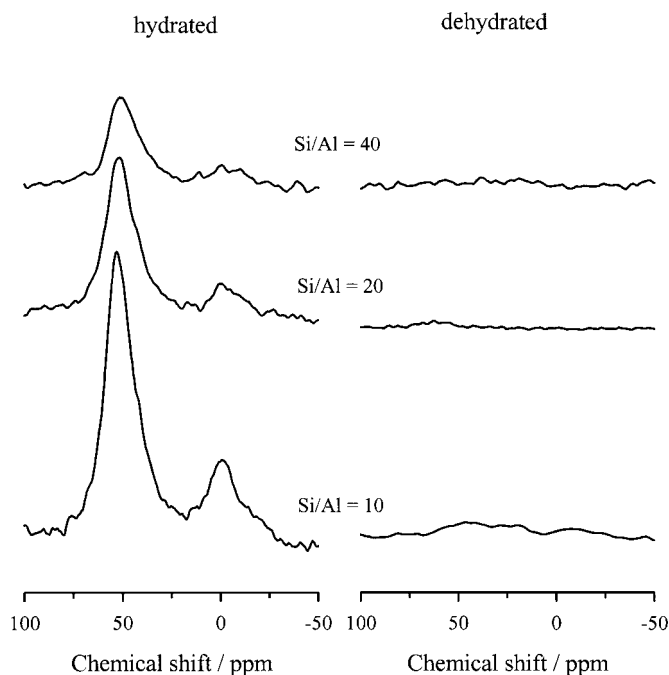


FIG. 7. MAS  $^{27}\text{Al}$  NMR spectra for calcined KIT-1 samples obtained by impregnation of an aqueous solution of  $\text{AlCl}_3$ . Hydrated samples were obtained by wetting with distilled water at room temperature after calcination at 823 K. The dehydration was performed by subsequent drying at 673 K in air.

change suggests that the coordination around the Al sites changed to lower symmetries that were difficult to detect by MAS  $^{27}\text{Al}$  NMR spectroscopy upon the complete dehydration. Thus, the loss of the NMR peak at 50 ppm could be due to the coordination change to three or a severely distorted tetrahedral site. Recently, a similarly three-coordinated Al site has been proposed to exhibit strong acidity in amorphous aluminosilicates (30). Since the silica frameworks of the mesoporous molecular sieves are likewise amorphous, it is reasonable that the catalytic activity of the postsynthesis samples may be due to formation of similar sites.

TABLE 2

Catalytic Conversion (%) of Benzyl Alcohol after 3 h  
in Friedel-Crafts Alkylation of Benzene

Sample	Si/Al ratio <sup>a</sup>			60
	9	19	38	
MCM-41		32	77	
KIT-1	9.5	51	65	95
MCM-48		48	45	

<sup>a</sup> Aluminum was incorporated by  $\text{AlCl}_3$  impregnation. The Si/Al ratio was determined by inductively coupled plasma emission spectroscopy. The molar composition of the reaction mixture was 1 benzene : 0.025 benzyl alcohol :  $0.65 \times 10^{-3}$  Al. The reaction was measured at 353 K with stirring under reflux conditions.

## CONCLUSION

The catalytic activity for the alkylation reaction depended significantly on synthesis methods rather than structural differences for KIT-1, MCM-41, and MCM-48. It is believed that the mesoporous materials have approximately the same intrinsic surface nature with regard to the catalytic reaction. Among the various synthesis routes used in the present work, postsynthesis impregnation of aqueous  $\text{AlCl}_3$  solution, followed by calcination, turned out to be the most effective means for increasing the catalytic activity. The Al sites thus generated were difficult to detect with MAS  $^{27}\text{Al}$  NMR unless the samples were sufficiently hydrated, supporting the possibility of three-coordinated catalytic sites.

## ACKNOWLEDGMENTS

The authors acknowledge financial support of the Korea Research Foundation in program year 1998.

## REFERENCES

1. Jansen, J. C., Creyghton, E. J., Njo, S. L., van Koningsveld, H., and van Bekkum, H., *Catal. Today* **38**, 205 (1997).
2. Clark, J. H., Cullen, S. R., Barlow, S. J., and Bastock, T. W., *J. Chem. Soc., Perkin Trans. 2* 1117 (1994).
3. Clark, J. H., Kybett, A. P., Macquarrie, D. J., Barlow, S. J., and Landon, P., *J. Chem. Soc., Chem. Commun.* 1353 (1989).
4. Barlow, S. J., Clark, J. H., Darby, M. R., Kybett, A. P., Landon, P., and Martin, K., *J. Chem. Res.* 74 (1991).
5. (a) Armengol, E., Corma, A., García, H., and Primo, J., *Appl. Catal. A* **149**, 411 (1997). (b) Gaare, K., and Akporiaye, D., *J. Mol. Catal. A* **109**, 177 (1996).
6. Kresge, C. T., Leonowicz, M. E., Roth, W. J., Vartuli, J. C., and Beck, J. S., *Nature* **359**, 710 (1992).
7. Beck, J. S., Vartuli, J. C., Roth, J. C., Leonowicz, M. E., Kresge, C. T., Schmitt, K. D., Chu, C. T.-W., Olson, D. H., Sheppard, E. W., McCullen, S. B., Higgins, J. B., and Schlenker, J. L., *J. Am. Chem. Soc.* **114**, 10834 (1992).
8. Armengol, E., Cano, M. L., Corma, A., García, H., and Navarro, M. T., *J. Chem. Soc., Chem. Commun.* 519 (1995).
9. Luan, Z., Hartmann, M., Zhao, D., Zhou, W., and Kevan, L., *Chem. Mater.* **11**, 1621 (1999).
10. Yue, Y., Gédéon, A., Bonardet, J.-L., Melosh, N., D'Espinose, J.-B., and Fraissard, J., *Chem. Commun.* 1967 (1999).
11. He, N., Bao, S., and Xu, Q., *Appl. Catal. A* **169**, 29 (1998).
12. Corma, A., *Chem. Rev.* **97**, 2373 (1997).
13. Climent, M. J., Corma, A., Iborra, S., Navarro, M. T., and Primo, J., *J. Catal.* **161**, 786 (1996).
14. Dai, L. X., Hayasaka, R., Iwaki, Y., and Tatgumi, T., *Sogo Shikensho Henpo (Tokyo Daigaku Kogakubu)* **55**, 169 (1996).
15. De Goede, A. T. J. W., van der Lekj, I. G., van der Heijden, A. M., van Rantwijk, F., and van Bekkum, H., EP 952011325, 1995.
16. Mokaya, R., and Jones, W., *Chem. Commun.* 2185 (1997).
17. Mokaya, R., and Jones, W., *J. Mater. Chem.* **9**, 555 (1999).
18. Mokaya, R., *J. Catal.* **186**, 470 (1999).
19. Kawi, S., and Shen, S. C., *Stud. Surf. Sci. Catal.* **129**, 219 (2000).
20. Ryoo, R., Kim, J. M., Ko, C. H., and Shin, C. H., *J. Phys. Chem.* **100**, 17718 (1996).
21. Kim, J. M., Jun, S., and Ryoo, R., *J. Phys. Chem. B* **103**, 6200 (1999).
22. Ryoo, R., Joo, S. H., and Kim, J. M., *J. Phys. Chem. B* **103**, 7435 (1999).
23. Ryoo, R., Ko, C. H., and Park, I.-S., *Chem. Commun.* 1413 (1999).
24. Ryoo, R., and Jun, S., "Abstract of the 7th Korea-Japan Symposium on Catalysis," pp. 38-39. Chonnam National University, Kwangju, 1999.
25. Ryoo, R., Jun, S., Kim, J. M., and Kim, M. J., *Chem. Commun.* 2225 (1997).
26. Kruk, M., Antochshuk, V., Jaroniec, M., and Sayari, A., *Langmuir* **13**, 6267 (1997).
27. Kruk, M., Jaroniec, M., and Sayari, A., *J. Phys. Chem. B* **103**, 10670 (1999).
28. Luan, Z., Cheng, C.-F., He, H., and Klinowski, J., *J. Phys. Chem.* **99**, 10590 (1995).
29. Kim, J. M., Kim, S. K., and Ryoo, R., *Chem. Commun.* 259 (1998).
30. Fraile, J. M., Garcia, J. I., Mayoral, J. A., Pires, E., Salvatella, L., and Ten, M., *J. Phys. Chem. B* **103**, 1664 (1999).